2019

A peptide-based vaccine for Mycobacterium avium subspecies paratuberculosis

Gaber S. Abdellrazeq
Washington State University, Pullman & Alexandria University

Mahmoud M. Elnaggar
Washington State University, Pullman &Alexandria University

J. P. Bannantine
USDA-ARS, National Animal Disease Center, john.bannantine@usda.gov

David A. Schneider
Washington State University, Pullman & USDA, ARS, Animal Disease Research Unit

Cleverson D. Souza
Washington State University, Pullman

See next page for additional authors

Vaccine 37 (2019) 2783–2790

Contents lists available at ScienceDirect

Vaccine

journal homepage: www.elsevier.com/locate/vaccine

A peptide-based vaccine for *Mycobacterium avium* subspecies *paratuberculosis*

Gaber S. Abdellrazeq [a,b], Mahmoud M. Elnaggar [a,b], John P. Bannantine [c], David A. Schneider [a,d], Cleverson D. Souza [e], Julianne Hwang [e], Asmaa H.A. Mahmoud [a,f], Victoria Hulubei [a], Lindsay M. Fry [a,d], Kun-Taek Park [g], William C. Davis [a,*]

[a] Department of Veterinary Microbiology and Pathology, Washington State University, Pullman, WA, USA
[b] Department of Microbiology, Faculty of Veterinary Medicine, Alexandria University, Egypt
[c] USDA, ARS, National Animal Disease Center, Ames, IA, USA
[d] USDA, ARS, Animal Disease Research Unit, Pullman, WA, USA
[e] Department of Veterinary Clinical Sciences, Washington State University, Pullman, WA, USA
[f] Veterinary Quarantine of Alexandria, General Organization for Veterinary Services, Ministry of Agriculture, Egypt
[g] Department of Biotechnology, Inje University, Injero 197, Kimhae-si, Gyeongsangnam-do, Republic of Korea

ARTICLE INFO

Article history:
Received 15 August 2018
Received in revised form 26 March 2019
Accepted 14 April 2019
Available online 16 April 2019

Keywords:
Zoonotic pathogen
Mycobacterium avium subspecies *paratuberculosis*
Propidium monoazide
Flow cytometry
Intracellular killing
Monocyte derived dendritic cells
Cytotoxic T cells
Bovine

ABSTRACT

Recent efforts to develop a live attenuated vaccine against *Mycobacterium avium* subsp. *paratuberculosis* (*Map*), the causative agent of Johne's disease (JD), revealed *relA* is important in *Map* virulence. Deletion of the *relA* gene impairs the ability of *Map* to establish a persistent infection. Analysis of the basis for this observation revealed infection with a *relA* deletion mutant (Δ*relA*) elicits development of cytotoxic CD8 T cells (CTL) with the ability to kill intracellular bacteria. Further analysis of the recall response elicited by Δ*relA* vaccination showed a 35 kDa membrane peptide (MMP) is one of the targets of the immune response, suggesting it might be possible to develop a peptide-based vaccine based on MMP. To explore this possibility, ex vivo vaccination studies were conducted with MMP alone and incorporated into a nanoparticle (NP) vector comprised of poly (D, L-lactide-co-glycolide) and monophosphoryl lipid A (PLGA/MPLA). As reported, ex vivo vaccination studies showed CD8 CTL were elicited with classic and monocyte derived dendritic cells (cDC and MoDC) pulsed with MMP alone and incorporated into a PGLA/MPLA vector. Incorporation of MMP into a NP vector enhanced the ability of CD8 CTL to kill intracellular bacteria. The findings indicate incorporation of MMP into a PGLA/MPLA nanoparticle vector is one of the possible ways to develop a MMP based vaccine for Johne's disease.

1. Introduction

Mycobacterium avium subsp. *paratuberculosis* (*Map*) is a zoonotic pathogen with a broad host range due to its ability to infect multiple species including humans [1,2]. Similar to *Mycobacterium tuberculosis* and *Mycobacterium bovis,* exposure leads to development of a latent infection under immune control, making it difficult to detect infected animals during the early stages of infection. This has led to the inadvertent introduction of *Map* into livestock worldwide through movement of latently infected animals, as clearly illustrated by the emergence of *Map* in livestock in the Czech Republic following the fall of Soviet Union in 1989 [3]. The inability to detect animals during the early stages of infection has emphasized the need to develop a vaccine that induces sterile immunity to control infection.

Some efficacy has been achieved with the use of killed vaccines, showing the potential of vaccination as a strategy to clear *Map* from livestock [4–8]. However, vaccination with killed vaccines does not elicit sterile immunity. Efforts are currently underway to determine if efficacy might be improved through the use of a live attenuated vaccine [9–13]. As part of an inter-institutional program to develop attenuated live vaccines, we used site-directed mutagenesis to evaluate the effect of deletion of specific genes on the immune response to Map [14]. Initial studies revealed one of three genes selected for analysis, *relA,* was unable to establish a persistent infection in two of the natural hosts, cattle and goats [15]. Examination at necropsy, revealed the Δ*relA* mutant could not establish a persistent infection in either species.

* Corresponding author at: Department Veterinary Microbiology/Pathology, PO 647040, Washington State Univ., Pullman, WA 99164-7040, USA.
E-mail address: davisw@wsu.edu (W.C. Davis).

https://doi.org/10.1016/j.vaccine.2019.04.040
0264-410X/

Clearance of this mutant was associated with development of an immune response that impaired the capacity of *Map* to establish an infection in vaccinated animals. Flow cytometric (FC) analysis of the recall response of peripheral blood mononuclear cells (PBMC) from vaccinated cattle showed vaccination elicited a proliferative response dominated by CD4 and CD8 T cells [15,16].

Two assays were developed to extend these findings. The first was designed to examine the functional activity of memory CD4 and CD8 T cells present in PBMC from vaccinated steers proliferating in response to stimulation of blood mononuclear cells (PBMC) and monocyte derived dendritic cells (MoDC) pulsed with antigen presenting cells (APC) i.e., conventional denedritic cells (cDC), present in peripheral blood, with live Δ*relA*. The second was a viability assay designed to distinguish live from dead bacteria in *Map*-infected macrophage (MΦ) target cells. Co-incubation of Δ*relA*-stimulated PBMC from vaccinated cattle, with MΦ infected target cells, revealed that stimulation with Δ*relA* elicited the development of CD8 cytotoxic T cells with ability to kill intracellular *Map*. Further analysis of the recall response revealed an equivalent response could be elicited with APC pulsed with Δ*relA* or a 35 kDa membrane peptide (MMP) [17]. This observation suggested that it might be possible to elicit the same CTL response with MMP alone, obviating the problems of using an attenuated live vaccine. To explore this possibility, studies were designed to examine the immune response to MMP ex vivo. We discovered that CTLs could be generated ex vivo with MMP alone. This was demonstrated by modifying the ex vivo functional assay to include two rounds of stimulation of PBMC with APC pulsed with MMP [17].

The current study was conducted to determine if MMP could be incorporated into a nano particle vector to develop a method for vaccine delivery in vivo. A vector comprised of poly (D,L-lactide-co-glycolide) and monophosphoryl lipid A (PLGA/MPLA) was examined for its potential use in a peptide-based vaccine for *Map* [18]. PGLA is a well characterized polymer that is now commercially available for use in vaccines [19]. MPLA is an endotoxin derivative used as a vaccine adjuvant that is also commercially available [20]. It binds specifically to the pro-inflammatory receptor TLR4 present on APC [21]. As reported in the presents study, we observed that the immune response to MMP was enhanced when incorporated into the PLGA/MPLA NP.

2. Material and methods

2.1. Animals

Six Holstein steers (12–18 months of age) were obtained from the Washington State University (WSU) *Map*-free dairy herd and used as a source of blood to conduct the studies described herein. The steers were maintained in an open feed lot by the college Animal Resource Unit staff. All protocols and procedures were approved by the WSU Institutional Animal Care and Use Committee (ASAF 4883).

2.2. Antigen preparation and construction of the PLGA/MPLA vector

The full length MMP, encoded by *MAP2121c*, was expressed with the maltose binding protein (MBP) in ClearColi BL21 (DE3) [22] and purified as previously described [23–25]. We optimized the coating of nanoparticals with recombinant *Map* proteins in a previous study and used those methods herein. [18]. Briefly, PLGA/MPLA MMP NPs were obtained by using the double emulsion water-in-oil-in-water (W/O/W) technique. Nine mg of PLGA 75:25 (Mn 25–35 kDa) (Polyscitech) was dissolved in 450 μL of chloroform and then 50 μL of 2 mg/mL MPLA (monophosphoryl lipid A) from *S. Minnesota* R595-TLR-based adjuvant (InvivoGen) in 1:4 methanol-chloroform mixture was added to the PLGA polymer solution for loading the PLGA NPs with MPLA at 1% w/v externally. Next 50 μL MMP protein (20 mg/mL) was added to create a oil-in-water (O/W) emulsion. For empty PLGA/MPLA NPs, 50 μL PBS buffer was added to the PLGA-MPLA mixture. The resultant was emulsified by sonication twice for 30 s each on ice using a Branson Ultrasonics Sonifier™ Cup Horn sonicator at an amplitude of 20%. The emulsion was added dropwise into 1 mL of 1% poly vinyl alcohol (PVA, Mw 31–50 kDa) (Aldrich) while being continuously vortexed. This second W/O/W emulsion was then sonicated three times for 40 s on ice at an amplitude of 40%. Then the emulsion was added dropwise into 5 mL PVA (1%) and stirred for 4 h to evaporate chloroform. Afterward, the mixture was centrifuged at 4 °C for 15 min at 15,000*g*. The supernatant was discarded. The NPs were washed three times by centrifugation at 4 °C for 15 min at 15,000g in distilled water. The NPs were resuspended by sonication following pelleting by centrifugation in each wash cycle. After the final washing the NPs were resuspended in 1 mL of water and freeze-dried. The morphology of the PLGA NPs was determined by scanning electron microscopy (SEM). Briefly, dried PLGA/MPLA preparations with or without MMP were applied onto a pin stub covered with double-sided carbon tape and then coated with 3.5 nm of platinum/palladium using a Cressington Sputter Coater. Images were taken using a FEI Quanta 200F SEM (Franceschi Microscopy and Imaging center, WSU, WA) at 5–10 kV. The PLGA NPs preparations sizes were then measured using ImageJ software (NIH, 1.48v). Polydispersibility and zeta potential were assessed by nanoComposix, Analytical Services in San Diego, CA. A protein assay kit (Pierce Biotechnology) was used for the quantification of MMP loading in PLGA NP preparations (%wt). Briefly, 2.5 g of PLGA NPs were dissolved in 0.2 mL of 0.1 M NaOH solution. After overnight incubation at 4 °C, the protein concentration was measured using a BCA protein assay kit according to the manufacturer's instructions. Sample absorbance was measured at 562 nm by means of a microplate reader (BioTek, Winooski). Empty PLGA NPs served as control. Protein encapsulation efficiency (EE), determine as the ratio of the protein content in the PLGA NPs divided by the total mass of protein used. A Limulus Amebocyte Lysate (LAL) kit (Pierce Biotechnology) was used for the determination of the MPLA LC (% wt) in the NPs. Accordingly, aqueous MPLA solutions were analyzed with LAL in a plate reader to set up a calibration curve. MPLA content in the PLGA NPs was calculated by subtracting the concentration of supernatant-containing MPLA from the starting concentration of MPLA in the formula. MPLA encapsulation efficiency was determined by the ratio of the measured MPLA concentration in the PLGA NPs to the total concentration of MPLA in the formula. The properties of NP constructs are listed in Table 1.

2.3. Bacteria and culture conditions

Cultures of *Map* wild type strain (K10) were prepared from single colonies in Middlebrook 7H9 broth (Difco, BD biosciences, USA) supplemented with 6.7% para-JEM GS (Trek Diagnostic Systems, OH), 2 μg/mL mycobactin J (Allied Monitor, MO, USA), and 0.05% Tween 80 (Sigma-Aldrich Corp.) as previously described [14,15]. The cultures were grown in flasks with occasional shaking at 37 °C. When broth cultures reached an OD_{600} of 0.6–0.8, master stocks from the upper half of the bacterial suspension were prepared for immediate use in each experiment. Bacterial stocks were disaggregated by passages through a 26-gauge needle three times to ensure they were dispersed as a predominant single-cell suspension. The concentration of bacteria in the final preparation was estimated based on the final OD_{600} value [14].

Table 1
Properties of PLGA NPs constructs used in this study.

Formulation	Hydrodynamic diameter (nm)	Zeta Potential (mV)	Polydispersity Index	Protein EE (%)	MPLA EE (%)
PLGA	431 SD ± 162	−14.8	0.141	–	–
PLGA/MPLA	400 SD ± 125	−8.58	0.947	–	94.8
PLGA/MPLA/MMP	864 SD ± 708.8	−23.0	0.67	93.21	93.21

EE = encapsulation efficiency, PLGA = poly (lactic-co-glycolic acid), MPLA = monophosphoryl Lipid, MMP = MAP recombinant peptide.

2.4. Generation of CTL, MoDC and MoMΦ

As illustrated in the flow diagram (Fig. 1), blood was collected twice to obtain PBMC to conduct the studies. Whole blood was collected from the jugular vein by venipuncture into bottles containing acid citrate dextrose (ACD). PBMC were isolated by density gradient separation using Ficoll-Paque™ (GE Healthcare Life Sciences, density 1.077).

Cytotoxic T-lymphocytes (CTL) were generated ex vivo from the blood of naïve steers as previously described [17]. In brief, blood was first collected to obtain: (1) monocyte-depleted PBMC (mdPBMC) that were stimulated with PLGA/MPLA NPs alone and PLGA/MPLA/MMP NPs processed and presented by circulating dendritic cells (cDC), and (2) monocytes that were stimulated with GM-CSF/IL-4 to generate immature monocyte-derived dendritic cells (MoDC) for use with MMP and NP constructs in the second week.

Magnetic microbeads, coated with a cross-reactive anti-human CD14 mAb, were used to isolate monocytes from PBMC by positive selection per the manufacturer's instructions (Miltenyi Biotec Ltd., CA), leaving behind the negatively selected mdPBMC containing cDC [26]. Purity, as assessed by FC with another anti-bovine CD14 mAb, CAM36A, was ~98% [27,28]. To generate the initial primed T cells, mdPBMC were added to wells of six well culture plates and cultured in 5 mL (2×10^6/mL) of complete culture medium (cRPMI) [RPMI-1640 medium with GlutaMAX™ (Life Technologies, CA, USA) supplemented with 10% calf bovine serum (CBS), 1 mM β-mercaptoethanol, 100 units/mL of penicillin G, and 100 μg/mL of streptomycin sulfate]. MMP (5 μg/mL), PLGA/MPLA NPs (25 μg/mL) and PLGA/MPLA-MMP NPs (25 μg/mL) were added to the cultures. The plates were incubated for 6 days at 37 °C, 5% CO_2.

Monocytes from the first blood draw were cultured in 3 mL of cRPMI in six well culture plates (2×10^6 per well) in the presence of a DC growth cocktail containing bovine GM-CSF and IL-4 according to the manufacturer's instructions (Kingfisher Biotech, MN, USA). On the third day, approximately half of the medium was replaced with fresh medium containing the cocktail and incubated an additional three days. On day seven, the MoDC cultures were washed three times with warm RPMI to remove non adherent and any dead cells. Three ml of fresh cRPMI was added. Then preparations of PLGA/MPLA NPs, MMP and PLGA/MPLA-MMP NPs were added as described above. The Ag-pulsed MoDC culture plates were centrifuged at 700*g* for five min prior to incubation at 37 °C with 5% CO_2. Following 3 h incubation, the excess of the Ag preparations was removed by washing three times with RPMI.

The primed mdPBMC were collected and subjected to density gradient centrifugation to remove dead cells, suspended in fresh cRPMI and added to their respective autologous Ag- pulsed MoDC (~2×10^6/mL in 5 mL of cRPMI) and cultured for an additional 6 days for the second round of Ag stimulation. Following collection, one set of cultures was used to phenotype the cells by FC. The second set was used to determine their functional activity using the CTL and bacterium viability assays as described in the following paragraph.

To generate MoMΦ for use as target cells, fresh PBMC, prepared from the second blood draw, were re-suspended in cRPMI, placed in 150 mm tissue culture plates and incubated overnight to allow adherence of monocytes as previously described [16,29]. Following removal of the majority of the non-adherent cells, the adherent cells were cultured for 4 days. For use, the differentiated MoMΦ were brought into suspension by incubating them on ice in the presence of EDTA in PBS (4 mL EDTA [250 mM stock in H_2O], 5 mL CBS, 91 mL PBS). The cells were washed by centrifugation and re-suspended in cRPMI, counted and then seeded into wells of 6 well plates (2×10^6/well). After an additional 2 days of culture, the MoMΦ cultures were washed three times with warm RPMI without antibiotics to remove any non-adherent and dead cells, leaving uniform lawns of cells. Fresh cRPMI with no antibiotics was added to each well to prepare the cell preparations for use in the viability assay.

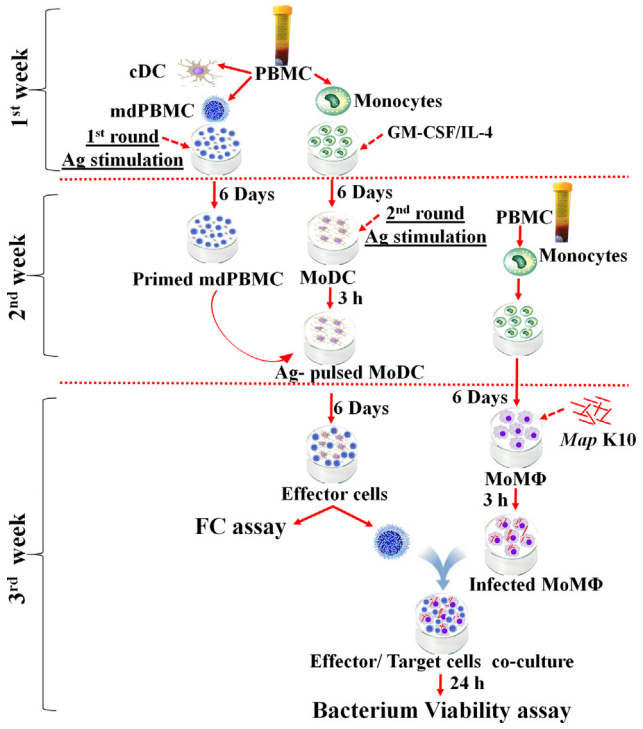

Fig. 1. Flow diagram for generating effector and target cells for use in the ex vivo assays. See methods for detail.

2.5. Bacterium viability assay

The bacterium viability assay was used as previously described (cite here) to compare the extent of intracellular killing of *Map* mediated by CTLs generated in response to APC pulsed with MMP alone or MMP incorporated into the PLGA/MPLA NP vector. In brief, MoMΦ in antibiotic free cRPMI were infected with *Map* K-10 at a multiplicity of infection (MOI) of 10:1. The culture plates were centrifuged at 700*g* for five minutes to maximize uptake of bacteria, then incubated at 37 °C, 5% CO_2 for 3 h. Extracellular bac-

teria were removed by washing 5 times with warm RPMI with no antibiotics. MdPBMC (Ag-primed or unprimed) were added to the cultures of infected MoMΦ. Two wells were used as controls, without addition of mdPBMC. All wells of mdPBMC/infected MoMΦ co-cultures and infected MoMΦ control cultures were incubated for 24 h, except cells in one control well that were lysed immediately following infection with *Map* using 0.01% saponin in H_2O. The pellets were re-suspended in 400 μL of H_2O in 1.5 mL translucent Eppendorf tubes and stored at − 20 °C for later treatment. At the end of incubation time, cells (including non-adherent and adherent) in all cultures were lysed and stored as described.

One μL of 20 mM propidium monoazide (PMA) working stock solution was added to each of 400 μL of the previously prepared cell lysates. The tubes were incubated for five minutes in the dark at room temperature using a tube rotator followed by a 5 min of light exposure using a halogen lamp with a 650 W bulb as described [17]. The cell pellets were obtained by centrifugation at 10 000*g* for five minutes.

In addition to the PMA-treated cell lysates, a set of controls were prepared for use as reference points when extrapolating the level of *Map* killing mediated by Ag specific effector T cells. This set of controls was made to contain *Map* mixed in five ratios, 100% live, 75% live/25% killed, 50%live/50% killed, 25% live/75% killed, and 100% killed. Aliquots of each preparation were added to the MoMΦ cultures at MOI of ten respectively and incubated for three h. The controls were treated with PMA as described [17].

DNA extraction from all PMA-treated tubes, including the mixed live/dead *Map* controls, was performed in duplicate according to the protocol for Gram-positive bacteria using DNeasy® Blood and Tissue kit (Qiagen, USA) following enzymatic lysis to facilitate breakdown of the *Map* cell wall as described by Park et al. [30]. The TaqMan Quantitative Real-Time PCR, targeting the single copy F57 gene specific for *Map* (F57 qRT-PCR) was used to determine the extent of intracellular *Map* killing relative to the controls based on the mean cycle threshold (C_T) as described by Kralik et al. [31] and Abdellrazeq et al. [17]. The reaction was performed according to Schönenbrücher et al. [32] using a StepOnePlus Real-Time PCR machine (Applied Biosystems, CA). *Map* gDNA prepared from pure culture was used to generate a standard curve with the F57 probe, made with 8 dilutions starting with 4×10^7 copies down to 4 copies. The total reaction volume was 25 μL including 5 μL of the DNA sample. The reactions were run for 40 cycles. The qRT-PCR conditions and sequences for primer and probe were the same as previously described [30]. The results were analyzed using StepOne Software v2.1 (Applied Biosystems, CA).

2.6. Flow cytometric analysis of the recall response

At the times indicated in the flow diagram (Fig. 1), a full set of mdPBMC (with and without Ags stimulation) were processed for FC analysis as previously described [17]. In brief, cells were subjected to density gradient centrifugation, washed once in PBS/ACD then re-suspended in serum-free RPMI and counted. Cells were distributed in a 96 well polystyrene V-shape bottom microplates (10^6 cells/well). Combinations of mAbs (Table 2), obtained from the WSU Monoclonal Antibody Center, were used to label cells. Data were collected on a FACSsort (BD Immunocytometry systems, San Jose CA) equipped with a Cell Quest software operating system or on a modified FACS Calibur DxP8 Analyzer (Cytek Biosciences, Inc. Fremont, CA) equipped with a Flow Jo Analysis software operating system. FCS Express software (DeNovo Software, Glendale, CA) was used for data analysis. The gating strategy used to collect the data is shown in Fig. 2. The flow cytometers were set to collect a minimum of 5×10^4 events. At the time of data analysis, FSC versus the memory marker (CD45R0) was used to determine the frequency of activated memory $CD4^+$ and $CD8^+$ T cells at the initiation of culture and following the first and second rounds of Ag stimulation.

2.7. Statistical analysis

Data were imported into SAS software (SAS for Windows version 9.3 and JMP version 12.0.1; SAS Institute Inc., Cary, NC) for statistical analysis and graphical presentation (means and standard deviations). A hierarchical mixed model (the generalized linear mixed model, or GLIMMIX, procedure) was used to analyze the effects of two stimulants (four levels defined by the absence, presence or combined presence of MMP and PLGA/MPLA NPs) on in vitro activation (proportional) of two types of T-cells ($CD4^+$ or $CD8^+$). The model was based on a binomial response distribution and Kenward-Roger degrees of freedom approximation, and residual error was treated as a random effect defined by subjects (T-cell type nested within blood-donor steers) and unstructured covariance matrix. A mixed model (GLIMMIX procedure) was also used to analyze the effects of in vitro CTL stimulation on macrophage intracellular MAP killing (estimated by C_T). The model was based on a Gaussian response distribution and Kenward-Roger degrees of freedom approximation, and residual error was treated as a random effect defined by subjects (blood-donor steers) and simple diagonal (variance component) covariance matrix structure. All post-hoc comparisons of simple effects (least squares means) were adjusted for multiple comparisons using the method of Holm-Tukey (overall $\alpha = 0.05$).

3. Results

Following our previous demonstration that comparable CD8 T cell responses could be elicited with either Δ*relA* or MMP processed and presented ex vivo by APC [17], studies were conducted to validate the response to MMP and explore the potential of a NP vector for testing MMP as a peptide-based vaccine. Preliminary experiments showed NP comprised of PGLA and MPLA could be prepared in a size range that is readily taken up by MoMΦ with no deleterious effects on viability. Further experiments demon-

Table 2
MAbs used in the present study.

mAb	Isotype	Specificity/Source	Fluorochrome	Labeling
CAM36A	IgG1	CD14 WSUMAC[a]	Alexa Fluor® 647	Indirect
CAM66A	IgM	CD14 WSUMAC[a]	PE	Indirect
209MD26A	IgG2a	CD209 WSUMAC[a]	PE CY5.5	Indirect
ILA11A	IgG2a	CD4 WSUMAC[a]	PE CY5.5	Indirect
CACT138A	IgG1	CD4 WSUMAC[a]	Alexa Fluor® 647	Indirect
7C2B	IgG2a	CD8 WSUMAC[a]	PE CY5.5	Indirect
CACT80C	IgG1	CD8 WSUMAC[a]	Alexa Fluor® 647	Indirect
ILA116A	IgG3	CD45R0 WSUMAC[a]	Alexa Fluor® 488; PE	Indirect

[a] WSUMAC = Washington State University Monoclonal Antibody Center.

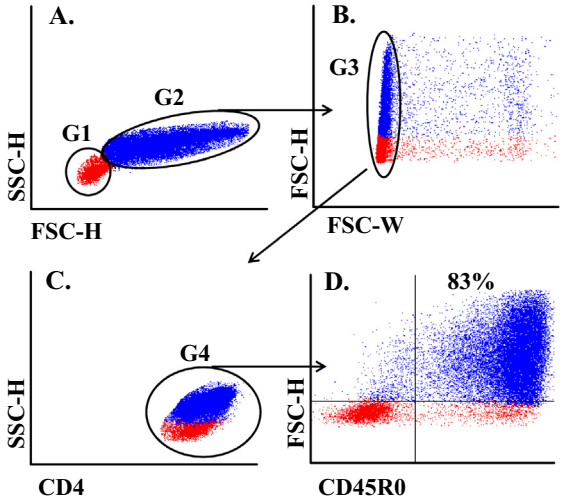

Fig. 2. Flow cytometric assay for phenotyping the effector T cell response to Ag-pulsed bDC/MoDC. (A) The gating strategy used to first identify the small lymphocytes (G1, color coded red) and large activated lymphocytes (G2, color coded blue) by forward scatter (FSC) and side scatter (SSC). (B) A third gate (G3) was placed on single cells using a pulse geometry gate (FSC-H vs FSC-W) to eliminate doublets. A fourth gate (G4) was placed on CD4 and CD8 T cells (CD4 cells in this illustration) to isolate activated cells for analysis. Using FSC vs CD45R0 (a memory marker) shows activated memory cells responded to Ag stimulation (upper right quadrant). Only the activated memory cells were considered for statistical analysis. (For interpretation of the references to color in this figure legend, the reader is referred to the web version of this article.)

strated candidate *Map*-derived peptides could be incorporated into the NP with high efficiency [18]. As part of the overall study design, cultures of mdPBMC were prepared with MMP alone and incorporated into the PLGA/MPLA NP. PLGA/MPLA NP alone was also included as a control to determine if MPLA alone had any effect on the functional activity of mdPBMC.

As shown in Fig. 3A and similar to results obtained in our previous studies [17], two rounds of stimulation of APC with MMP alone elicited robust CD4 and CD8 CTL proliferative responses ($P < 0.0001$, each). Stimulation with PLGA/MPLA NP alone also elicited a proliferative response in both CD4 and CD8 T cells ($P < 0.0001$, each) but with no CTL activity, as observed with infected macrophages incubated with unstimulated mdPBMC ($P = 0.2892$; Fig. 4. While a significant difference was not detected between the proliferative responses elicited by MMP alone and MMP incorporated into the PLGA/MPLA NP (CD4 T cells, $P = 0.6931$; CD8 T cells, $P = 0.9812$; Fig. 3B), there was a difference in killing activity: the CTL response elicited in mdPBMC stimulated with MoDC pulsed with PLGA/MPLA-MMP NP (Compare the red square MMP in the NP vector with the yellow square MMP alone in Fig. 4A) was significantly greater than the response to MMP alone ($P < 0.0001$; *yellow square in* Fig. 4A).

4. Discussion

Demonstrating the potential efficacy of experimental vaccines before testing in the field has been a major challenge because methods available for fully evaluating the immune response to vaccines have been limited for *Map* as well as other pathogens. In the course of our studies on the immunopathogenesis of JD, we have been able to overcome some of the difficulties encountered in analysis of the immune response to *Map* using the natural host and development of methods for testing the potential efficacy of candidate vaccines ex vivo. With the use of selective gating during flow cytometry, it is possible to isolate CD4 and CD8 memory T cells proliferating in response to Ags processed and presented by cDC in blood or MoDC ex vivo. This has facilitated analysis of signaling through APC that drives T cell differentiation during the primary immune response of naïve T cells and during the recall response of T cells, ex vivo or in vivo, with T cells from animals immunized with Ags of interest. Likewise, it allowed for the analysis of the effector activity of T cells proliferating in response to Ag stimulation. The adaptation of site directed mutagenesis allowed for selection of specific genes for deletion to determine the effect of deletion on the capacity of the mutant to establish a persistent infection [14]. Adaptation of a propidium-based viability assay to distinguish live from dead bacteria in a mixed population of live and dead bacteria obviated problems with culturing this slow growing pathogen to assess the activity of cytotoxic T cell activity against intracellular bacteria [17,31].

When we selected genes for analysis of the effect of gene deletion on survival in vivo, we were particularly interested in *relA*, a global regulator of multiple gene functions in bacteria [33]. Studies in mouse models demonstrated deletion greatly reduced survival in vivo, indicating deletion might in some way alter the immune response to *Map* [34,35]. This proved to be a correct assumption. Deletion of *Map* resulted in loss of the ability to establish a persistent infection. *RelA* appears to be the Achilles' heel of mycobacterial pathogens. Comparative studies are needed with wild type *Map* to identify the metabolic products associated with dysregulating the immune response that are not expressed when *relA* is deleted. What was revealed in our studies is that, in absence of the immunomodulatory products regulated by *relA*, it is possible for a protective immune response to develop against *Map*. Analysis of the recall response ex vivo demonstrated, inability of *Map* to establish a persistent infection, was associated with the development of cytotoxic T cells with the ability to kill intracellular bacteria. The immune response to the Δ*relA* mutant may include a response to multiple bacterial products that differ from the response elicited by wild type *Map*. Thus any of the products could be involved in eliciting a CTL response. Based on previous studies, we selected MMP as a start for dissecting the immune response to Δ*relA*. Initial studies had shown MMP is a virulence protein that enhances invasion of epithelial cells in the bovine intestine [36]. Increased levels of this protein were present under conditions that mimic the intestinal environment and, antibodies against this protein significantly inhibited cell invasion. The protein exists as part of a membrane complex containing other proteins including a cysteine desulfurase [37]. A strong antibody response is elicited early in the course of natural infection with *Map* [38]. As reported here, further analysis has now revealed the immune response also includes development of CTL with the ability to kill intracellular bacteria [17].

As a further step in exploring the potential of developing a peptide-based vaccine with MMP, studies were conducted to determine the potential of a nano particle vector to deliver the vaccine in vivo. We chose to use a well characterized NP, PLGA, to initiate the studies and included MPLA as a stimulant to target the use of CTLA-4 for Ag uptake [18]. The use of PLGA/MPLA alone, as one of the controls, showed it did have a stimulatory effect but the proliferating cells did not develop any CTL activity against *Map*. Consistent with studies with Δ*relA* and MMP alone, APC pulsed with PLGA/MPLA-MMP NP elicited a proliferative response equivalent to stimulation with MMP alone that included both CD4 and CD8 T cells. Although there was no detectable difference in the proliferative response, there was an increase in the CTL activity in mdPBMC stimulated with APC pulsed with MMP incorporated into a NP vector.

The ability to study the functional activity of CD4 and CD8 T cells proliferating in response to stimulation with APC pulsed with Ags ex vivo has afforded increased opportunities to evaluate the

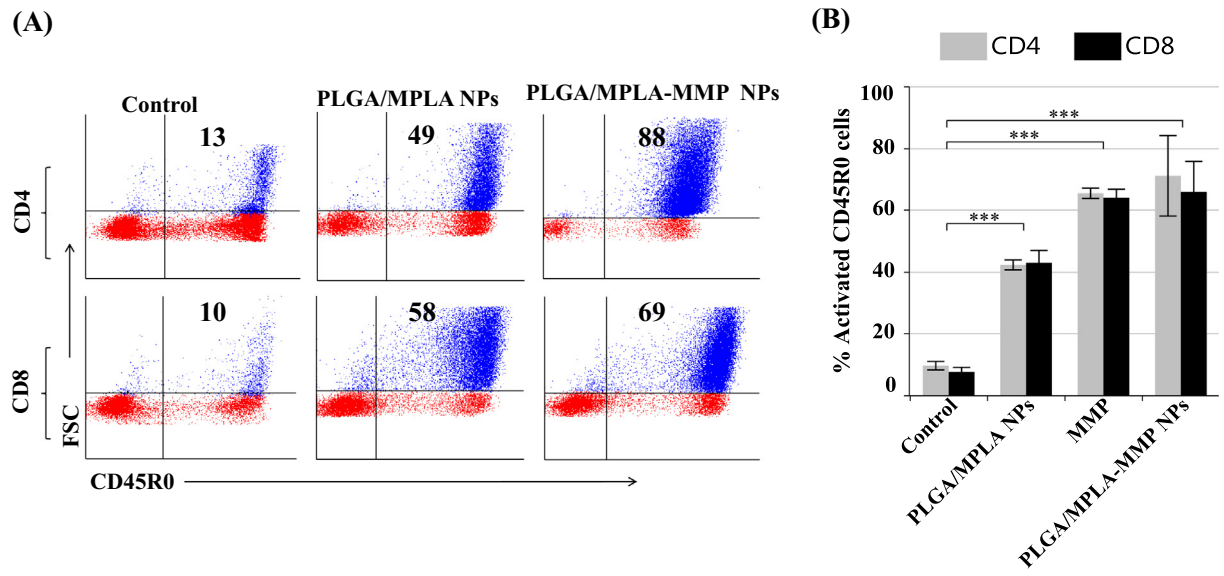

Fig. 3. The proliferative response of CD4 and CD8 T cells to MMP nanoparticles. (A) Representative FC profiles for CD4 and CD8 T cells cultured in medium alone (control) or stimulated with either PLGA/MPLA NP alone or PLGA/MPLA-MMP NP. (B) Summary of 6 replications of the FC assay comparing the percentage of activated memory CD4 and CD8 T cells in controls or in response to two rounds of stimulations with PLGA/MPLA NP, MMP or PLGA/MPLA-MMP NP. Data were imported into SAS software for statistical analysis and graphical presentation (means and standard deviations). See methods for detail. No proliferative response was observed in both CD4 and CD8 T cells in control cultures. MMP alone elicited a robust CD4 and CD8 proliferative response ($P < 0.0001$, each). PLGA/MPLA NP alone also elicited a proliferative response in both CD4 and CD8 T cells ($P < 0.0001$, each). No significant difference was detected between the proliferative responses elicited by MMP alone or MMP incorporated into the PLGA/MPLA NP (CD4 T cells, $P = 0.6931$; CD8 T cells, $P = 0.9812$).

efficacy of candidate vaccines before testing in vivo. Use of the methods in the study of the immune response to *Map* has allowed us to follow up studies on a *relA* deletion mutant and show one of the targets of the immune response, MMP, is a good candidate for the development of a peptide-based vaccine for JD. It is not clear at this time, what the best vector should be to obtain an efficacious

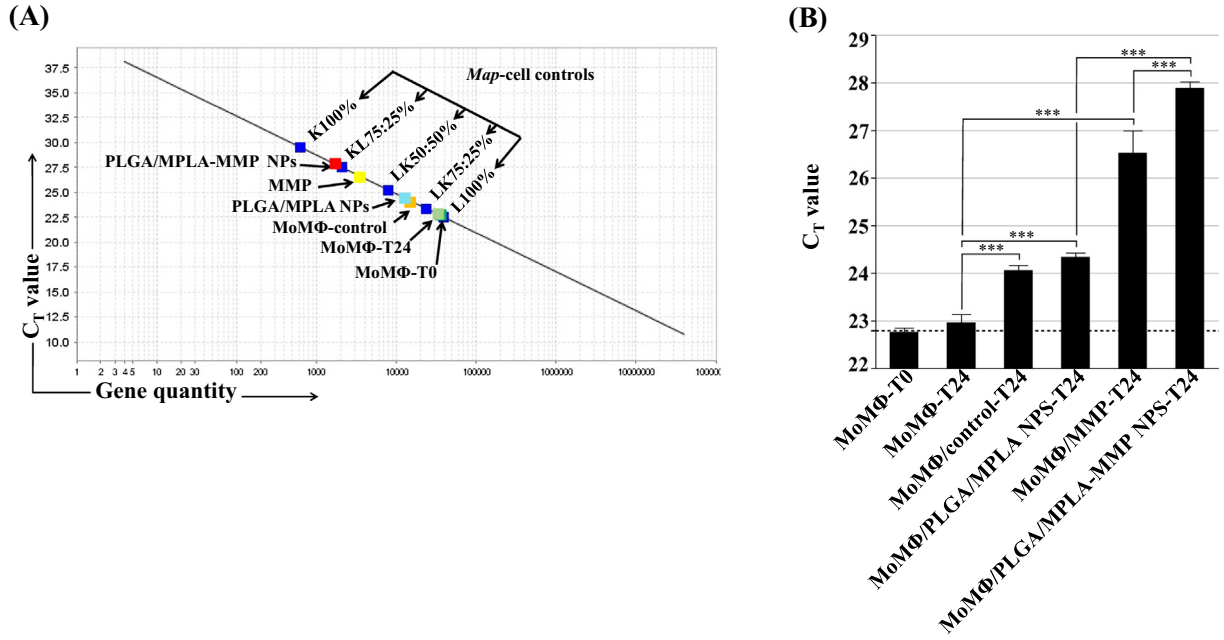

Fig. 4. CTL kill *Map* in infected MoMΦ. (A) Standard curve of the TaqMan F57 qRT-PCR. Five blue square data points represent *Map* DNA controls from 2×10^7 *Map* mixtures (live and dead), incubated for 3 h with MoMΦ and then treated with PMA. C_T values represent average of duplicate preparations of DNA. Killing activity for all cell treatments are represented by C_T values and plotted using different colors on the standard curve, which is marked by blue data points. Higher C_T values indicate higher intracellular killing activity and vice-versa. (B) Summary of 6 replications of the viability assay comparing killing activities in all cell treatments based on C_T values. Mean and standard deviation for each treatment effect ($n = 6$ independent experiments). Data were imported into SAS software for statistical analysis and graphical presentation (means and standard deviations). See methods for detail. No apparent CTL killing activity in mdPBMC stimulated with MoDC pulsed with PLGA/MPLA NP alone, similar to activity observed in infected macrophages incubated with unstimulated mdPBMC ($P = 0.2892$). CTL killing activity elicited in mdPBMC stimulated with MoDC pulsed with PLGA/MPLA-MMP NP was significantly greater than the response to MMP alone ($P < 0.0001$). (For interpretation of the references to color in this figure legend, the reader is referred to the web version of this article.)

response in vivo. Receptor usage during uptake and processing of MMP by APC may be essential for driving CTL differentiation. Uptake of Ags through TLRs may be critical in priming APCs to drive effector T cell differentiation towards protective and non-protective immune responses [39]. TLR2 usage has been associated with activation pathways leading to a non-protective immune response to *Map* [40]. TLR4 hasn't been examined by our group but data suggest usage might be associated with induction of protective immunity [41]. In the present study, a nonspecific enhancement of the CD4 and CD8 T cell proliferative response was observed when MPLA was included in a NP vector. It appears this nonspecific stimulatory effect did not alter the proliferative response to MMP when incorporated into a PLGA NP vector. However, there was an increase in CTL activity. Further studies are now needed to determine whether there is a modulatory effect of MPLA on Ag processing and presentation by APC in vivo.

Competing interests

The authors declare that they have no competing interests.

Authors' contributions

GSA and WCD conceived the study. GSA, JPB and WCD participated in the design of the protocol to conduct the studies. JPB participated in the development and use of the *Map* major membrane protein (MMP). CDS and JW participated in the construction of NP vectored MMP. GSA conducted the experiments. MME and VH participated in the conduct of the experiments. GSA and DAS participated in statistical analysis of the data. GSA, MME, AHAM, KTP, WCD, JPB, CDS, DAS, and LMF participated in the writing and interpretation of the results. WCD, JPB and CDS obtained the funding for the project. WCD oversaw and participated in all aspects of the study. All authors read and approved the final manuscript.

Acknowledgments

The authors wish to acknowledge the excellent technical support and animal care provided by Emma Karol and her staff, and Bruce Mackey (USDA-ARS-Pacific West Area) for review of the statistical methods applied. The results of this study were presented as a poster in ESVCP 2017 congress, London (UK), orally in ACVP 2017, Vancouver, (Canada), and orally in 14th International Colloquium on Paratuberculosis, Riviera Maya, Mexico.

Funding

Support was provided by the Wash. State Univ. Monoclonal Antibody Center.

Appendix A. Supplementary material

Supplementary data to this article can be found online at https://doi.org/10.1016/j.vaccine.2019.04.040.

References

[1] Singh SV, Kumar N, Sohal JS, Singh AV, Singh PK, Agrawal ND, et al. First mass screening of the human population to estimate the bio-load of *Mycobacterium avium* sub-species *paratuberculosis* in North India. JPHE 2014;6:20–9.
[2] Singh SV, Kuenstner JT, Davis WC, Agarwal P, Kumar N, Singh D, et al. Concurrent resolution of chronic diarrhea likely due to Crohn's disease and infection with *Mycobacterium avium* paratuberculosis. Front Med (Lausanne) 2016;3:49.
[3] Hruska KPI. Crohn's disease and related inflammatory diseases: from many single hypotheses to one "superhypothesis". Vet Med 2014;59:583–630.
[4] Singh K, Chandel BS, Chauhan HC, Dadawala A, Singh SV, Singh PK. Efficacy of 'indigenous vaccine' using native 'Indian bison type' genotype of *Mycobacterium avium* subspecies paratuberculosis for the control of clinical Johne's disease in an organized goat herd. Vet Res Commun 2013;37:109–14.
[5] Alonso-Hearn M, Molina E, Geijo M, Vazquez P, Sevilla IA, Garrido JM, et al. Immunization of adult dairy cattle with a new heat-killed vacine is associated with longer productive life prior to cows being sent to slaughter with suspected paratuberculosis. J Dairy Sci 2012;95:618–29.
[6] Juste RA, Alonso-Hearn M, Molina E, Geijo M, Vazquez P, Sevilla IA, et al. Signoficant reduction in bacterial shedding and improvement in milk production in dairy farms after the use of a new inactivated paratuberculosisd vaccine in a field trial. BMC Res Notes 2009;2:233. 6 pages.
[7] Harris NB, Barletta RG. *Mycobacterium avium* subsp. paratuberculosis in veterinary medicine. Clin Microbiol Rev 2001;14:489–512.
[8] Sweeney RW, Whitlock RH, Bowersock TL, Cleary DL, Meinert TR, Habecker PL, et al. Effect of subcutaneous administration of a killed *Mycobacterium avium* subsp paratuberculosis vaccine on colonization of tissues following oral exposure to the organism in calves. Am J Vet Res 2009;70:493–7.
[9] Bannantine JP, Hines 2nd ME, Bermudez LE, Talaat AM, Sreevatsan S, Stabel JR, et al. A rational framework for evaluating the next generation of vaccines against *Mycobacterium avium* subspecies paratuberculosis. Front Cell Infect Microbiol 2014;4:126.
[10] Bannantine JP, Everman JL, Rose SJ, Babrak L, Katani R, Barletta RG, et al. Evaluation of eight live attenuated vaccine candidates for protection against challenge with virulent *Mycobacterium avium* subspecies paratuberculosis in mice. Front Cell Infect Microbiol 2014;4:88.
[11] Chen J-W, Faisal SM, Chandra S, McDonough SP, Moreira MAS, Scaria J, et al. Immunogenicity and protective efficacy of the *Mycobacterium avium* subsp. paratuberculosis attenuated mutants against challenge in a mouse model. Vaccine 2012;30:3015–25.
[12] Faisal SM, Chen JW, Yan F, Chen TT, Useh NM, Yan W, et al. Evaluation of *Mycobacterium avium* subsp. paratuberculosis leuD mutant as vaccine candidate against challenge in a caprine model. Clin Vaccine Immunol 2013;20:572–81.
[13] Settles EW, Kink JA, Talaat A. Attenuated strains of *Mycobacterium avium* subspecies paratuberculosis as vaccine candidates against Johne's disease. Vaccine 2014;32:2062–9.
[14] Park KT, Dahl JL, Bannantine JP, Barletta RG, Ahn J, Allen AJ, et al. Demonstration of allelic exchange in the slow-growing bacterium *Mycobacterium avium* subsp. paratuberculosis, and generation of mutants with deletions at the pknG, relA, and lsr2 loci. Appl Environ Microbiol 2008;74:1687–95.
[15] Park KT, Allen AJ, Bannantine JP, Seo KS, Hamilton MJ, Abdellrazeq GS, et al. Evaluation of two mutants of *Mycobacterium avium* subsp. paratuberculosis as candidates for a live attenuated vaccine for Johne's disease. Vaccine 2011;29:4709–19.
[16] Park KT, ElNaggar MM, Abdellrazeq GS, Bannantine JP, Mack V, Fry LM, et al. Phenotype and function of CD209+ bovine blood dendritic cells, monocyte-derived-dendritic cells and monocyte-derived macrophages. PLoS ONE 2016;11:e0165247.
[17] Abdellrazeq GS, Elnaggar MM, Bannantine JP, Park KT, Souza CD, Backer B, et al. A Mycobacterium avium subsp. paratuberculosis relA deletion mutant and a 35 kDa major membrane protein elicit development of cytotoxic T lymphocytes with ability to kill intracellular bacteria. Vet Res 2018;49:53.
[18] Souza CD, Bannantine JP, Brown WC, Norton MG, Davis WC, Hwang JK, et al. A nano particle vector comprised of poly lactic-co-glycolic acid and monophosphoryl lipid A and recombinant *Mycobacterium avium* subsp paratuberculosis peptides stimulate a pro-immune profile in bovine macrophages. J Appl Microbiol 2017;123(1):54–65.
[19] Danhier F, Ansorena E, Silva JM, Coco R, Le Breton A, Preat V. PLGA-based nanoparticles: an overview of biomedical applications. J Control Release 2012;161:505–22.
[20] Fichter M, Dedters M, Pietrzak-Nguyen A, Pretsch L, Meyer CU, Strand S, et al. Monophosphoryl lipid A coating of hydroxyethyl starch nanocapsules drastically increases uptake and maturation by dendritic cells while minimizing the adjuvant dosage. Vaccine 2015;33:838–46.
[21] Wang DB. Monophosphoryl lipid A is an lipopolysaccharide-derived Toll-like receptor 4 agonist which may improve Alzheimer's disease pathology. Expert Opin Biol Ther 2013;13:1639–41.
[22] Planesse C, Nativel B, Iwema T, Gasque P, Robert-Da Silva C, Viranaicken W. Recombinant human HSP60 produced in ClearColi BL21(DE3) does not activate the NFkappaB pathway. Cytokine 2015;73:190–5.
[23] Bannantine JP, Li L, Mwangi M, Cote R, Raygoza Garay JA, Kapur V. Complete genome sequence of *Mycobacterium avium* subsp. paratuberculosis, isolated from human breast milk. Genome Announc 2014;2.
[24] Bannantine JP, Lingle CK, Stabel JR, Ramyar KX, Garcia BL, Raeber AJ, et al. MAP1272c encodes an N1pC/P60 protein, an antigen detected in cattle with Johne's disease. Clin Vacc Immunol 2012;19:1043–92.
[25] Bannantine JP, Stabel JR, Bayles DO, Geisbrecht BV. Characteristics of an extensive *Mycobacterium avium* subspecies paratuberculosis recombinant protein set. Protein Expr Purif 2010;72:223–33.
[26] Park KT, Burnett S, Davis WC. Development and characterization of a monoclonal antibody specific for bovine CD209. Vet Immunol Immunopathol 2015;163:216–20.
[27] Park KT, Seo KS, Godwin NA, Van Wie BJ, Gulbahar MY, Park YH, et al. Characterization and expression of monoclonal antibody-defined molecules

on resting and activated bovine alphabeta, gammadelta T and NK cells. Vet Immunol Immunopathol 2015;168:118–30.
[28] Elnaggar MM, Abdellrazeq GS, Mack V, Fry LM, Davis WC, Park KT. Characterization and use of new monoclonal antibodies to CD11c, CD14, and CD163 to analyze the phenotypic complexity of ruminant monocyte subsets. Vet Immunol Immunopathol 2016;178:57–63.
[29] Corripio-Miyar Y, Hope J, McInnes CJ, Wattegedera SR, Jensen K, Pang Y, et al. Phenotypic and functional analysis of monocyte populations in cattle peripheral blood identifies a subset with high endocytic and allogeneic T-cell stimulatory capacity. Vet Res 2015;46:112.
[30] Park KT, Allen AJ, Davis WC. Development of a novel DNA extraction method for identification and quantification of *Mycobacterium avium* subsp. paratuberculosis from tissue samples by real-time PCR. J Microbiol Meth 2014;99:58–65.
[31] Kralik P, Nocker A, Pavlik I. Mycobacterium avium subsp. paratuberculosis viability determination using F57 quantitative PCR in combination with propidium monoazide treatment. Int J Food Microbiol 2010;141(Suppl. 1): S80–6.
[32] Schonenbrucher H, Abdulmawjood A, Failing K, Bulte M. New triplex real-time PCR assay for detection of *Mycobacterium avium* subsp. paratuberculosis in bovine feces. Appl Environ Microbiol 2008;74:2751–8.
[33] Hauryliuk V, Atkinson GC, Murakami KS, Tenson T, Gerdes K. Recent functional insights into the role of (p)ppGpp in bacterial physiology. Nat Rev Microbiol 2015;13:298–309.
[34] Dahl JL, Kraus CN, Boshoff HIM, Doan B, Foley K, Avarbock D, et al. The role of RelMtb-mediated adaptation to stationary phase in long-term persistence of *Mycobacterium tuberculosis* in mice. Proc Natl Acad Sci USA 2003;100:10026–31.
[35] Weiss LA, Stallings CL. Essential roles for *Mycobacterium tuberculosis* Rel beyond the production of (p)ppGpp. J Bacteriol 2013;195:5629–38.
[36] Bannantine JP, Huntley JFJ, Miltner E, Stabel JR, Bermudez LE. The Mycobacterium avium subsp. paratuberculosis 35 kDa protein plays a role in invasion of bovine epithelial cells. Microbiology 2003;149:2061–9.
[37] Leite FL, Reinhardt TA, Bannantine JP, Stabel JR. Envelope protein complexes of *Mycobacterium avium* subsp. paratuberculosis and their antigenicity. Vet Microbiol 2015;175:275–85.
[38] Li L, Munir S, Bannantine JP, Sreevatsan S, Kanjilal S, Kapur V. Rapid expression of *Mycobacterium avium* subsp. paratuberculosis recombinant proteins for antigen discovery. Clin Vacc Immunol 2007;14:102–5.
[39] Dowling JK, Mansell A. Toll-like receptors: the swiss army knife of immunity and vaccine development. Clin Transl Immunol 2016;5:e85.
[40] Souza C, Davis WC, Eckstein TM, Srteevatsan S, Weiss DJ. Mannosylated lipoarabinomannans from *Mycobacterium avium* subsp. Paratuberculosis alters the inflammatory response by bovine macrophages and suppresses killing of *Mycobacterium avium* subsp. Avium organisms. PLoS ONE 2013;8:e75924.
[41] Zhang Y, Zhu X, Feng Y, Pang W, Qi Z, Cui L, et al. TLR4 and TLR9 signals stimulate protective immunity against blood-stage *Plasmodium yoelii* infection in mice. Exp Parasitol 2016;170:73–81.